Proceedings of the
44th IEEE Conference on Decision and Control, and
the European Control Conference 2005
Seville, Spain, December 12-15, 2005

Loop Shaping Robust Control for Scaled Teleoperation System

Moussa Boukhnifer, Antoine Ferreira, Jean Guy Fontaine

Laboratoire Vision et Robotique, Université d'Orléans,
10 Boulevard Lahitolle, 18020 Bourges, France,
moussa.boukhnifer@ensi-bourges.fr

***Abstract*- This paper presents a force-reflecting macro-micro teleoperator operating in a remote micro environment. Due to the transmission time delay, it is very difficult to ensure the stability. Then, in order to manipulate micro-object it is inevitable to consider the scaling effect problem between worlds with different physical characteristics, with minimal loss of physical information and robustness against variation of scaling gains. Accordingly, in this paper, the controllers are designed based on the framework H_∞ Loop Shaping procedure approach. This approach allows a convenient means to trade-off the robustness for a pre-specified time-delay margin, variation of force scaling factors and uncertainties in environment modeling. The validity of the proposed method is demonstrated by simulations.**

1. INTRODUCTION

The stability-performance trade-off is the main determinant of the control design for teleoperation systems. Recent controller designs using robust H_∞ control theory and μ-synthesis/analysis are very effective for macro scale teleoperation [1][2][3][4]. In order to resolve the problem of robust stability and performance of bilateral micromanipulation in the presence of a multi-objective problem: time delay, variation of force scaling, uncertainty in the microenvironment and uncertainties in the master-slave models. In a previous study, the design of H_∞, H_2 controllers with on-line control of the scaling parameters for a network-based force-reflecting teleoperation has been examined [5][6]. However, weighting function selection is not an easy task and the order of the final controller, which is designed by H_∞, H_2 mixed-sensitivity optimisation is usually high.

In this work, we extend the loop shaping approach, originally proposed in [7] and further developed in [8] and [9] which incorporates characteristics of both loop shaping and H_∞ design. Specifically, we make use of the so-called normalized coprime factor H_∞ robust stabilization problem which has been solved in [10][11] and is equivalent to the gap metric robustness optimisation as in [12]. The design technique has two main stages : 1) loop shaping is used to shape the nominal plant singular values to give desired open-loop properties at frequencies of high and low loop gain; 2) the normalized coprime factor H_∞ problem mentioned above is used to robustly stabilize this shaped plant. The paper is organized as follows. In section 3, the design of the H_∞ loop shaping controller with compensation of time-delay is discussed. In Section 4, the developed micro-teleoperation system is introduced, and various simulations are given.

2. ROBUST CONTROL METHODOLOGY

A. Robust Controller Design using Normalized Coprime Factor

We define the nominal model of the system to be controlled starting from the coprime factors on the left: $G = \tilde{M}^{-1} \cdot \tilde{N}$. Then a perturbed model is written (see Fig .1)

$$\tilde{G} = (\tilde{M} + \Delta_M)^{-1} \cdot (\tilde{N} + \Delta_N) \qquad (1)$$

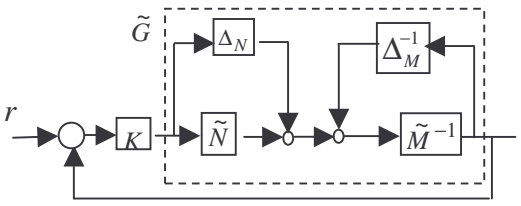

Fig.1 : Coprime factor robust stabilization problem.

where $\tilde{G}$ is a left coprime factorization (LCF) of G, and Δ_M, Δ_N are unknown and stable transfer functions representing the uncertainty. We can then define a family of models with the following expression :

$$\xi_\varepsilon = \left\{ \tilde{G} = (\tilde{M} + \Delta_M) \cdot (\tilde{N} + \Delta_N) : \left\| (\Delta_M \ \Delta_N) \right\|_\infty \langle \varepsilon_{\max} \right\} \qquad (2)$$

where $\varepsilon_{\max}$ represent the margin of maximum stability. The robust problem of stability is thus to find the greatest value of $\varepsilon = \varepsilon_{\max}$, such as all the models belonging to ξ_ε can be stabilized by the same corrector K. The problem of robust stability H_∞ amounts finding $\gamma_{\min}$ and $K(s)$ stabilizing $G(s)$ such as:

$$\left\| (K)\cdot(I-K\cdot G)^{-1}(IG) \right\|_{\infty} = \gamma_{\min} = \frac{1}{\varepsilon_{\max}} \qquad (3)$$

However, Mc Farlane and Glover [12] showed that the minimal value γ of is given by :

$$\gamma_{\min} = \varepsilon_{\max}^{-1} = \sqrt{1+\lambda_{\sup}(XY)} \qquad (4)$$

where $\lambda_{\sup}$ indicates the greatest eigenvalue of *XY*. Moreover, for any value $\varepsilon\langle\varepsilon_{\max}$ a corrector stabilizing all the models belonging to ξ_{ε} is given by:

$$K(s) = B^T X (sI - A + BB^T X - \gamma^2 ZYC^T C)^{-1} \gamma^2 ZYC^T$$
$$\text{where} \quad Z = (I + YX - \gamma^2 I)^{-1} \qquad (5)$$

where *A, B* and *C* are state matrices of the system defined by the function *G,* and *X*, *Y* are the positive definite matrices and solution of the Ricatti equation :

$$A^T X + XA - XB^T BX + C^T C = 0$$
$$AY + YA^T - YC^T CY + BB^T = 0 \qquad (6)$$

B. The Loop-Shaping Design Procedure

Contrary to the approach of Glover-Doyle , no weight function can be introduced into the problem. The adjustment of the performances is obtained by affecting an open modeling (loop-shaping) process before calculating the corrector. The design procedure is as follows :

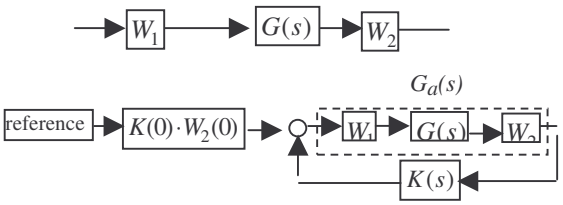

Fig.2 : The loop-shaping design procedure.

- We add to the matrix *G*(*s*) of the system to be controlled a pre-compensator W_1 and/or a post-compensator W_2, the singular values of the nominal plant are shaped to give a desired open-loop shape. The nominal plant *G*(*s*) and shaping functions W_1 and W_2 are combined in order to improve the performances of the system such as $G_a = W_1 G W_2$ (see Fig.2). In the monovariable case, this step is carried out by controlling the gain and the phase of $G_a(jw)$ in the Bode plan.

- From coprime factorizations of $G_a(s)$, we apply the previous results to calculate $\varepsilon_{\max}$, and then synthesize a stabilizing controller *K* ensuring a value of ε slightly lower than $\varepsilon_{\max}$

$$\left\| \begin{pmatrix} I \\ K \end{pmatrix} \cdot (I - K\cdot W_2 \cdot G \cdot W_1)^{-1} (I \quad W_2 \cdot G \cdot W_1) \right\|_{\infty} = \gamma = \frac{1}{\varepsilon} \qquad (7)$$

- The final feedback controller is obtained by combining the H_∞ controller *K* with the shaping functions W_1 and W_2 such that $G_a(s) = W_1 G W_2$ (See Fig.2).

3. Design of H_∞ Loop Shaping Controller

A. Bilateral System

Figure 3 illustrates the block diagram of the bilateral controller system with the time-delay parameters and fixed scaling factors. A generalized scaled bilateral manipulator is characterized by a fixed geometric/ kinematic scaling factor, k_p, and a fixed force scaling factor, k_f. Using the scaling factors, the relationships between the master and slave in position and force are :

$$x_m = k_p^{-1} x_s$$
$$f_h = k_f f_s \qquad (8)$$

where x_m and x_s are the position command from the master and the slave position, respectively; f_h and f_s are the operator force command and the external force from the slave to the master. The transfer functions on position of the master and the slave are represented by $P_m(s)$ and $P_s(s)$ such that:

$$P_m(s) = \frac{1}{m_m s^2 + k_m s + b_m} \;,\; P_s(s) = \frac{1}{m_s s^2 + k_s s + b_s} \qquad (9)$$

where m_m , m_s denote the mass of master and slave, k_m and k_s the compliance coefficients and b_m and b_s denote the viscosity coefficients, The terms, f_h and f_e are the operation force and the reaction force while the output master and slave positions are, respectively, x_m and x_s. The slave is in contact with the environment S_e. G_s represents the slave which is in contact with the environment S_e and the velocity of the slave is controlled by K_s. The time-delay from the master to the slave, and vice-versa, are represented by e^{-sT1} and e^{-sT2}. Consider H_∞ Loop Shaping design of controllers for the master and slave for free motion. Let K_m and K_s denote free motion controllers for the master and slave, respectively.

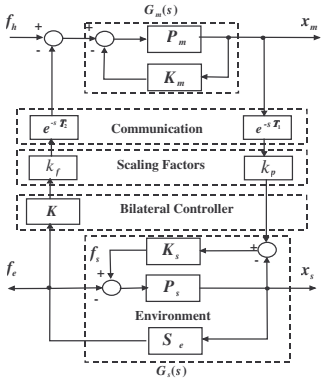

Fig.3: Bilateral controller with communication channel and scaling factors.

B. H_∞ Loop Shaping Controller of the Master

The synthesis of the master controller K_m is obtained according to the implementation shown in the Fig.2. using the command *ncfsyn* of MATLAB μ-Analysis and Synthesis toolbox [13]. The controller K_m is obtained by combining the pre-filter W_{1m} and the post-filter W_{2m}. The pre-filter and post-filter are used to shape the open-loop plant to achieve a desired frequency responses according to some well defined design specifications such as bandwidth and steady-state error [14]. In order to ensure a high gain in low frequencies and a low gain in high frequencies and to obtain a high performance and a good robustness, we add the following weight functions

$$W_{1m} = \frac{9 \cdot s + 5}{0.02 \cdot s + 0.02}, W_{2m} = 1$$

The Fig.4 shows the frequency responses of the master system , the $W_{m1}.P_m.W_{m2}$ and the open-loop system $W_{m1}.P_m.W_{m2}.K_m$. The results show that the open-loop remains close to the step response obtained after the choice of the shaping functions and K_m ensures correct margins of stability.

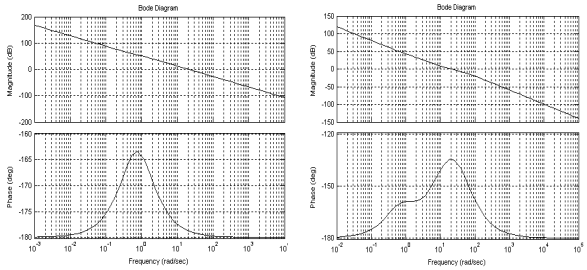

(a) (b)

Fig.4 : Open-loop responses of (a) W_{m1} P_m W_{m2} and (b) W_{m1} $P_m W_{m2}$ K_m

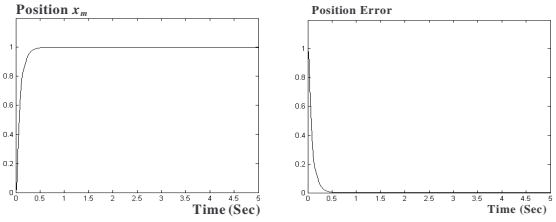

Fig.5 : Step response of the master : x_m ,x_m-f_h.

C. H_∞ Loop Shaping Controller of the Slave

The synthesis of the slave controller K_s is obtained according to the implementation in the Fig.2. The slave is adjusted by the shaping functions W_{s1}, W_{s2}. The Fig.6 shows the frequency responses of the compensated slave system $W_{s1}.P_s.W_{s2}$ and the open-loop system $W_{s1}.P_s.W_{s2}.K_s$. Taking into account the low frequency behavior of the slave, with the same method we chose the shaping functions $W_{s1,}$ W_{s2} as follows:

$$W_{s1} = \frac{585000 \cdot s + 5}{s} \quad , \quad W_{s2} = 1$$

By using the command *ncfsyn* of MATLAB μ-Analysis and Synthesis Toolbox, the controller K_s ensures correct margins of stability in Fig. 6 and the slave position follows the master position in Fig.7.

D. H_∞ Loop Shaping Bilateral Controller

In order to synthesize the robust bilateral controller, we have used a Padé approximation for the communication time-delay $W_T(s)=e^{-sT}$. Time-delay variations are infinite-dimensional in polynomial space and cannot be represented exactly in the model. A Padé all-pass approximation has been used, such as:

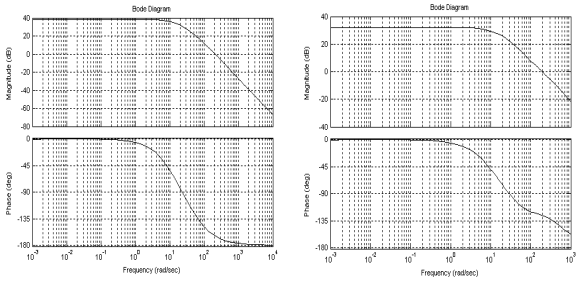

(a) (b)

Fig.6: Open-loop responses of (a) W_{1S} $P_S W_{2S}$ and (b) W_{1S} $P_S W_{2S}$ K_S.

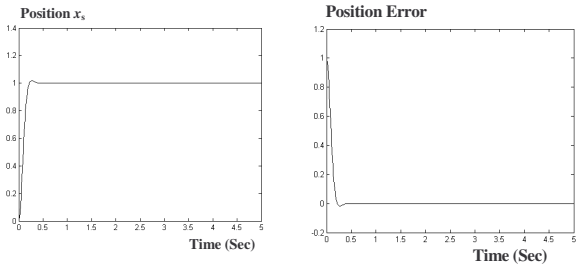

Fig.7 : Step response of slave : x_s ,x_s-x_m

$$W_T(s) = e^{-sT} = \frac{e^{-sT/2}}{e^{+sT/2}} = \frac{1 - \frac{sT}{2} - \frac{(sT)^2}{8} - \frac{(sT)^3}{48}}{1 + \frac{sT}{2} + \frac{(sT)^2}{8} + \frac{(sT)^3}{48}} \qquad (10)$$

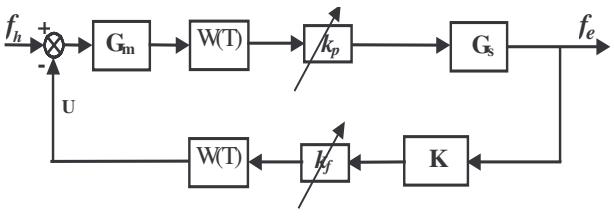

Fig.8: Bilateral controller with padé approximation of time delay.

a different value might be used. In our study, the microenvironment is modeled as a spring and a damper:

$$S_e = \frac{K_e}{s} + B_e s \qquad (11)$$

The H_∞ loop shaping bilateral controller design, given in Fig.8, is defined by the closed loop transfer function:

$$F_L(G,K) = \frac{k_p W_1 G_m G_s W_T W_2}{1 + k_f k_p W_1 K G_m G_s W_T W_2} \quad (12)$$

where G_m : loop transfer function around master

$$\mathbf{G}_m = \frac{A \cdot P_{ma}}{P_{ma} \cdot K_m + 1} \quad (13)$$

G_s: loop transfer function around slave

$$\mathbf{G}_s = \frac{B \cdot K_s \cdot P_{sa} \cdot S_e}{P_{sa} \cdot (S_e + K_s) + 1} \quad (14)$$

P_{ma}: loop shaping for master

$$P_{ma} = W_{m1} P_m W_{m2}, \quad A = K_m(0) \cdot W_{m2}(0)$$

P_{sa}: loop shaping for slave

$$P_{sa} = W_{s1} P_s W_{s2}, \quad B = K_s(0) \cdot W_{s2}(0)$$

The controller K is obtained by combining the pre-filter W_1 and the post-filter W_2. the pre-filter and post-filter are used to shape the open loop plant to achieve a desired frequency responses according to some well defined design specifications such as bandwidth and steady-state error. In order to ensure a high gain in low frequencies and a low gain in high frequencies and to obtain a high performance and a good robustness, we add the following weight functions :

$$W_1 = \frac{0.1 \cdot s + 0.5}{0.2 \cdot s} \quad ; \quad W_2 = 0.5$$

The Fig.9 shows the frequency responses of the system global G where $G=G_m G_s W_T$, the $W_1.G.W_2$ and the open-loop system $W_1.G.W_2.K$. The results show that the bode diagram obtained after the choice of the shaping functions and K ensures correct margins of stability.

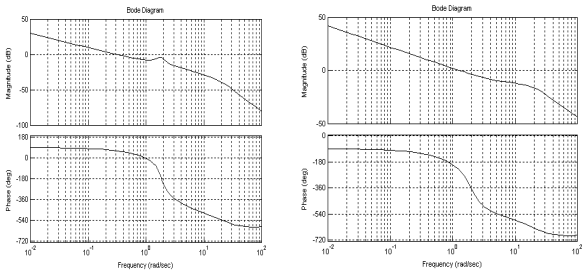

(a) (b)

Fig.9: Diagrams bode of (a) W_1 GW_2 K (b) W_1 GW_2

4. STABILITY ROBUSTNESS ANALYSIS

The analysis of the characteristic equation (12) shows that the denominator depends on the master and slave plants, global and local control, scaling gains of K_p , K_f , environment S_e and the communication time delay W_T. The two primary objectives of this design are robust stabilization and disturbance rejection. The global stability analysis is discussed in the following.

A. Feasible Scale Region

The region of stable operation in the space formed by the position scaling factor and force scaling factor is analyzed through the pole location criteria.

From the denominator of (12), we can observe that the scaling gains of k_p and k_f are in the product form $r_0 = k_p k_f$. By integrating (13) and (14) into (12), we can plot root locus of the system with respect to r_0. If we look the root locus diagram for a time-delay of W_T=2sec (Fig.10), the system is stable for all r_0 less than $r_0 = r_0^C = 2.1$ where r_0^C is called the upper bound of scaling product. It should be noted that r_0^C value increases as the time delay decreases allowing a wider feasible range of as shown in Table I.

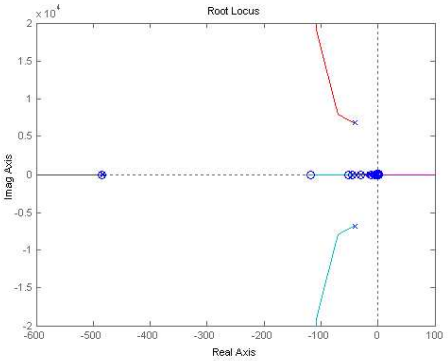

Fig.10: Root locus for a time delay of W_T= 2sec.

Table I: Upper bound values of the product of scaling r_0.

T(Sec)	2	1.75	1.5	1.25	1	0.5	0.25
r_0^C	2.1	2.37	2.81	3.3	4.22	7.77	11.1

In the scaled teleoperation, the feasible region of scaling of position and force should be known for several reasons such as safety and full use of the system. So far, there have been few papers showing how feasible operation region depends on position and force scaling factors [15]. Figure 11 shows stable scaling zone of position and force with a communication time-delay showing wider feasible range, and the upper bound of scaling gain product of position and force

We identified the stable feasible region of scaled teleoperation in terms of force and position scaling based on the characteristic Eq.(12) when the communication time-delay is varying from 0 to 2 sec. The curve shows the boundary of stability of position scaling k_p and force k_f. The upper high corner of the plot is the unstable region and the opposite lower corner is stable one. The key idea from this figure is that the constant value of the product of position and force scaling gain is the critical line of stability .

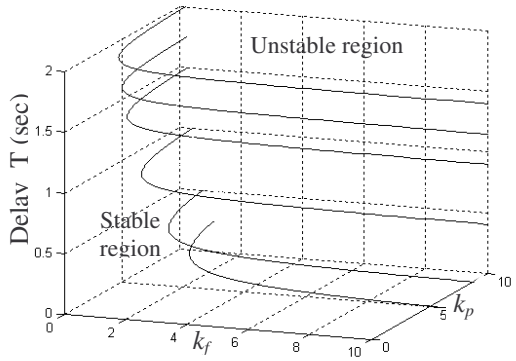

Fig.11: Zoom of stable scaling zone of position and force.

B. Environment Uncertainties

At the micro scale, the microenvironment is strongly subjected to disturbances and uncertainties according to the operating conditions. The approach of loop-shaping has the advantage of a relatively straightforward definition of the control objective, in a manner consistent with the identification uncertainty. More specifically, because the nominal stiffness of the microenvironment is postulated to be very uncertain, it is desired to robustly stabilize the plant for a range of stiffnesses, and to ensure that the closed-loop damping is at an acceptable level. The following environment variations are considered :

$$S_e \in \{(B_e + K_e / s): 0 \le B_e \le \infty, 0 \le K_e \le \infty\} \qquad (15)$$

The range of *Se* represents environments from zero to infinite stiffness and damping. The synthesized corrector ensures the robust stability for all the models *G* which can be stabilized by the same corrector and check the robustness condition $\|F_L(G,K)\|_\infty < \gamma$. In our case, the bilateral controller check the following expression:

$$\left\| \frac{k_p W_1 G_m G_s W_2 W_T}{1 + k_f k_p W_1 K G_m G_s W_2 W_T} \right\|_\infty \le \varepsilon_{\max}^{-1} \qquad (16)$$

The upper bounds are determined systematically by varying the parameter K_e while B_e is kept constant. We found a stability margin value of ε_{max}=0.34 which represents a robust stability indicator. The stability margin ε_{max} is always less than 1 and values of ε_{max} below 0.3 generally indicates good robustness margins. Finally, the H_∞ norm minimization of the closed-loop transfer functions defined in (16) achieves a good balance of the sensitivity and complementary functions so as to improve the overall system robustness against parameter variations such as coefficients of stiffness K_e in the environment, as well as the disturbance rejection performances against external disturbance and sensor noise. Such robustness was experimentally validated by repeating the closed-loop transfer function measurements with the same shaped bilateral controller, but with a decreased environment stiffness of 500 Nm and an increased environment stiffness of 2750 Nm, respectively. The robustness condition (16) is checked for the values K_e < 1750, we show the margin gain and the margin phase are negatives for the values K_e > 2250 *N.m* (Fig.12). The shaped micro-teleoperation system clearly maintains the nominally stability robustness for microenvironments stiffnesses lower than K_e<*1750* Nm.

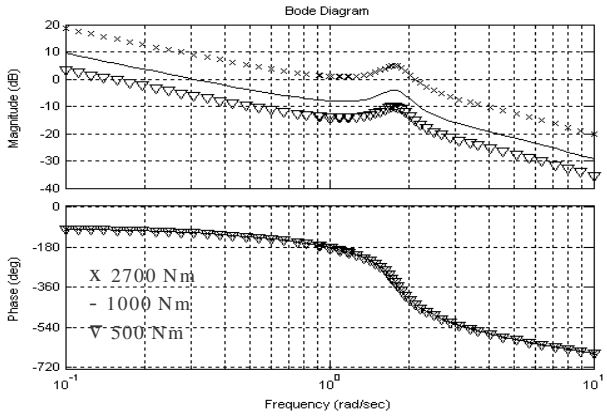

Fig.12: Closed-loop transfer function of the shaped bilateral controller for an environment stiffness K_e=500, 1000 and 2750 N.m.

5. CASE STUDY AND DISCUSSION

To illustrate the behaviour of the micro-teleoperation system and to confirm the findings of the previous section, the bilateral controller *K(T1+T2)* has been designed using robust control and μ-Analysis and Synthesis Toolbox from MATLAB *(ncfsyn).* Table II gives the parameters of simulation. The set of simulations of Fig.13.a and Fig.13.b shows the force step response without time delay for different values of scaling factors. The results demonstrate the excellent force tracking of the proposed teleoperation controller under variation of the scaling factors. The operator has regulated the optimum scaling parameters to (k_f=100, $k^{-1}{}_p$=100) for hard contact and (k_f=1000, $k^{-1}{}_p$=1000) for a soft contact in order to improve the direct force-reflection from the microenvironment.

TABLE II : SIMULATION PARAMETERS

Master	$m_m = 1$	k_m=0	b_m=0
Slave	$m_s = 4.88$	k_s=0.512.10^5	b_s=0.232.10^8
Environment		$S_e = 1000/s + 0.3$	

The simulations presented in Fig.14.a and Fig.14.b show the step response for the force in the case of variation of the operating environment. In both cases, the proposed bilateral controller design ensures the robust stability of the force against strong variations of the environment stiffness k_e (±50%). Fig.15.a and Fig.15.b show respectively the results of simulation for a time delay of T=2sec using Padé approximation and in the presence of the scaling factors for hard contact (k_f=100, $k^{-1}{}_p$=100) and soft contact (k_f=1000, $k^{-1}{}_p$=1000). The force felt is closely following the one sampled from the microgripper. Even if the transmission round trip time delays (T=2 Sec), the system maintains stability.

6. CONCLUSION

The Loop Shaping Design Procedure *(LSDP)* using H_∞ synthesis has been applied for controller design for a bilateral force-reflecting teleoperator in micro environment. That the value of scaling product, r_0 can be an index of the system stability is supported by [16]. But this approach does not take into account communication time-delay, non-identical master and slave manipulators, and environment uncertainty terms. The system is designed to function when there is pre-specified upper bound on the communication time delay (round-trip of 2 sec). The design of a task-based H_∞ Loop Shaping controller allows the time communication delay, the system has maintained the stability. In comparison to other robust H_∞ and H_2 controller designs [5][6], the selection of the weighting functions in H_∞ loop-shaping controller design is sample as the weighting functions are chosen according to some well-defined system specifications such as bandwidth and steady-state error requirement. In addition, the H_∞ loop-shaping controller can be found without any iterative computation.

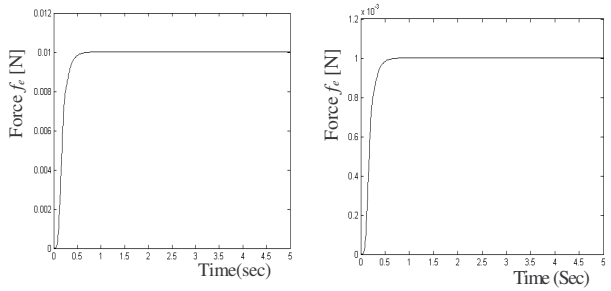

Fig.13: Step response of the force with no time-delay (a) ($k^{-1}{}_p$=k_f=100). (b) scaling factors ($k^{-1}{}_p$=k_f=1000).

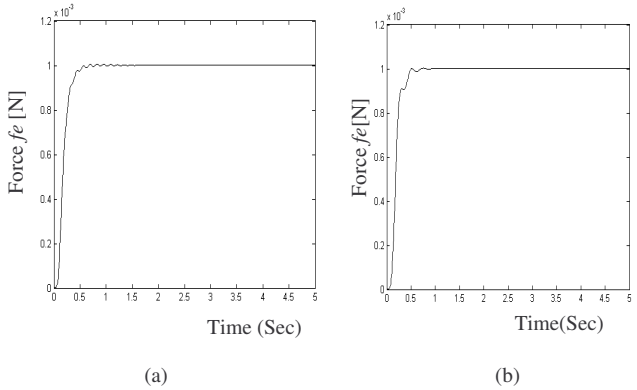

Fig.14: Step response of the force with no time-delay *($k^{-1}{}_p$=k_f =1000)* (a) with 50% increase of K_e.(b) with 50% reduction of K_e.

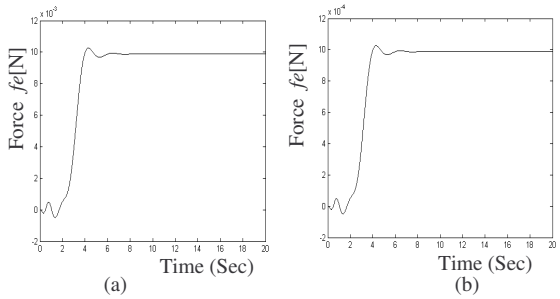

Fig.15: Closed-loop step response when the delay (T=2 sec) is simulated as a Padé approximation and (a) scaling factors ($k^{-1}{}_p$=k_f =100)., (b) scaling factors ($k^{-1}{}_p$=k_f=1000).

7. REFERENCES

[1]: Z. Hu, S.E. Saculdean, P.D. Loewen, "Robust controller design for teleoperation systems", *IEEE Int. Conf. On Systems, Man and Cybernetics*, vol.3, 1995, pp.2127-2132.

[2]: H. Kazeroni, T.-I. Tsay, K. Hollerbach, "A controller design framework for telerobotic systems", *IEEE Trans. on Control Systems Technology*,vol.1, 1993, pp.50-62.

[3]: G.M.H. Leung, B.A. Francis, J.Apkarian, "Bilateral controller for teleoperators with time-delay via μ-synthesis*", IEEE Trans. on Rob.&Autom*, vol.11, No.1, 1995, pp.105-116.

[4]: J. Yan, S.E. Saculdean, "Teleoperation controller design using H_∞ optimization with application to motion scaling", *IEEE Trans. on Contr. Sys. Tec.*, vol.4, No.3, 1996, pp.244-258.

[5]: M.Boukhnifer, A.Ferreira, "Scaled Teleleoperation Controller Design for Micromanipulation over Internet", *IEEE Int. Conf. On Robotics and Automation*, New-Orleans, May 2004, pp.4577-4583.

[6]: M.Boukhnifer, A.Ferreira, "H_2 Optimal Controller Design for Micro-Teleoperation with Delay", *IEEE/RSJ Int. Conf. on Intelligent Robots and Systems*, Sendai, September 2004, pp.224-229.

[7]: D.Mc Farlane, K. Glover, and M. Noton,"Robust stabilization of a flexible space- platform: An H_∞ coprime factors" in *Proc. IEEE Contr. Conf.,* 1988*,* Oxford, expanded in CUED Internal Rep CUED/E-INFENG/TR.5,1988.

[8]: D.Mc Farlane, K. Glover," An H_∞ design procedure using robust stabilization of normalized coprime factors" in proc. *IEEE Conf. Decision Contr*, Austin,TX,1988.

[9]: D.Mc Farlane, K. Glover, "Robust controller design using normalised coprime factor plant descriptions", *lecture Notes in Control and information Sciences*, Vol. 138, New York: Springer Verlag,1989.

[10]: K. Glover and D.Mc Farlane, "Robust stabilization of normalized coprime factors: An explicit H_∞ solution " in Proc. 1988 *Amer Contr., Conf.*,Atlanta,GA,1988.

[11]: K. Glover and D.Mc FArlane," Robust Stabilization of normalized coprime factor plant descriptions with H_∞ bounded uncertainly", *IEEE Trans. Auto , Contr*., Vol. 34, pp..821-830,Aug.1989

[12]: D.Mc Farlane, K Glover, "A loop shaping design procedure using H∞ synthesis", *IEEE Tran. on Automatic Control* , Vol 37 , pp. 759-769, 1992**.**

[13]: G. J. Balas, J. C. Doyle, K. Glover, A. Packard, and R. Smith,μ-*Analysis and Synthesis Toolbox*. Natick, MA: The MathWorks, Inc, 1994.

[14]: P. Lundstrom, S. Skogstad, Z.C. Wang, "Weight selection for H-infinity and mu-control methods: insights and examples from process control," *Workshop on H_∞ control*, Brighton, U.K, pp.139-157, 1991.

[15]: B. Hannaford, "Stability and performance tradeoffs in bilateral telemanipulation", *IEEE Int. Conf. on Robotics and Automation*, pp.1764-1767, 1989.

[16]: D.Y. Hwang, B. Hannaford, "Modeling and stability analysis of a scaled telemanipulation system", *IEEE Int. Workshop on Robots and Human Communication,* pp..32-37, 1994.